EFFECT OF Li CONTENT ON AGING RESPONSES AND MECHANICAL PROPERTIES OF AN Al-Mg-Si ALLOY

B. C. Wei*, Z. Huang*, Y. G. Zhang*, C. Q. Chen*, O. Reixach, V. Ji****

*Department of Materials Science and Engineering,
Beijing University of Aeronautics & Astronautics, Beijing, CHINA
**Laboratoire de Microstructure et Micromecanique des Materiaux,
Ecole Nationale Superieure des Arts et Metiers, Paris, FRANCE

ABSTRACT The effect of Li content on the aging precipitation and mechanical properties of Al-Mg-Si alloy was investigated. It was found that the ordered δ' phase becomes the predominant precipitate and no G.P. zones of Mg_2Si forms in 1.7%Li and 2.6%Li containing alloys at peak aging condition. Furthermore, the addition of 1.7% and 2.6%Li showed realy different influence on the strength and elongation of the Al-Mg-Si alloy. The 1.7%Li containing alloy showed a much lower strength and better elongation than the base alloy, owing to the limited precipitation of δ' phase. While, the 2.6%Li containing alloy showed a stronger aging response and higher tensile strength than the base alloy due to the excessive precipitation of δ'.

Keywords: *Al-Li-Mg-Si alloys, aging precipitation, mechanical properties, microstructures*

1. INTRODUCTION

The application of lighter advanced material in aircraft is an efficient way to reduce the structural weight and improve the effective load. Replacement of the conventional aluminum alloys currently used in aircraft structures with the low density high stiffness Al-Li base alloys could achieve weight saving of at least 10~15%[1]. Therefore, a considerable research has been made for these Lithium-containing aluminum alloys, and much progress has been made in defining the physical and mechanical metallurgy, in commercial alloy and process development, and in aerospace applications. A wide range of alloy series has been studied during this period. Most of the development work has concerned Al-Li-Cu-Mg, Al-Cu-Li and Al-Mg-Li series alloys [2,3]. However, much less attention has been paid to the 6000-Li (Al-Mg-Si-Li) series [4-6], although 6000 series alloys are important and widely used commercial alloy. The purpose of the present research is to investigate the influence of both 2.6% and 1.7% Lithium contents on the precipitation behaviors and mechanical properties of Al-Mg-Si alloy.

2. EXPERIMENTAL PROCEDURE

The chemical compositions of the alloys investigated are given in Table 1. The alloys were prepared from high purity metals, melted under argon atmosphere, homogenized at 803K for 24 hours, forged and rolled to 3 mm sheet. Specimens were solution heat treated at 813K for 30 minutes, and aged at 443K or 453K in silicon oil bath immediately after cold water quenching.

Table 1 Chemical composition of the alloys (wt.%)

Alloy No.	Li	Mg	Si	Cr	Fe	Al
A	—	0.68	0.78	0.21	<0.05	Bal.
B	1.7	0.66	0.80	0.22	<0.05	Bal.
C	2.6	0.62	0.81	0.22	<0.05	Bal.

The hardness was determined by the Vickers test using a 5 kg load, and tensile tests were carried out on Inston-4507 using specimens with 20 mm gauge length and the tensile axis parallel to the rolling direction.

The transmission electron microscopy (TEM) was performed on a H-800 operating at 150 KV with the foil normal to the through-thickness direction of the sheet. A S-5800 scanning electron microscopy (SEM) was employed to characterize the fractured surfaces of the failed tensile specimens.

3. RESULTS

3.1 Aging hardening

Aging curves were obtained by measuring the Vickers hardness of alloys as a function of aging time. Figure 1(a, b) shows the aging response of all three at 443 K and 453 K respectively. The response to 443K provided good control of aging at reasonable aging times. This was the basis for selection of 443 K as the temperature for most of the subsequent aging treatments.

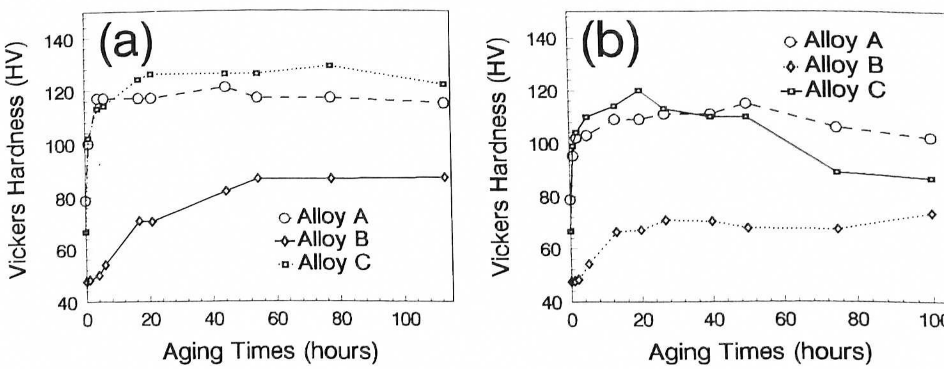

Fig. 1 Age-hardening curves of the alloys at (a) 443K; (b) 453K

It can be seen from Fig. 1 that alloys with different Li content show very different aging response. Alloy A (free from Li) reaches a peak hardness of 121HV after 10 hours at 443K. Alloy B (containing 1.7%Li) shows a quite slower aging response and considerably lower hardness compared with alloy A, and it does not attain a peak hardness even up to 100 hours. Alloy C (Containing 2.6%Li) exhibits the strongest age-hardening response, and it obtains a peak hardness of 130HV in 24 hours at 443K.

3.2 Microstructures

Fig.2a shows the TEM image of alloy A after peak aging (443K, 24h). The needle-shaped G.P. zones aligned along <100>$_{Al}$ orientation are the dominant precipitates. As the aging proceeds to the overaged condition (100h, Fig.2b), growth of the needles in matrix and Si particles on grain boundaries can be observed. The present of Mg_2Si precipitate free zones adjacent to grain boundary is visible too.

The ordered δ′ phase is the predominant precipitates in Li containing alloys. Fig.2(c, d) show the precipitation features of alloy B after aging for 80 hours. It can be seen that δ′ phases are nearly homogeneous within the matrix except for PFZ's near grain boundaries, and a few large particles, which were conformed to be unsoluted LiSiAl phase, distribute primarily within matrix. Few precipitates on the grain boundary can be seen in alloy B.

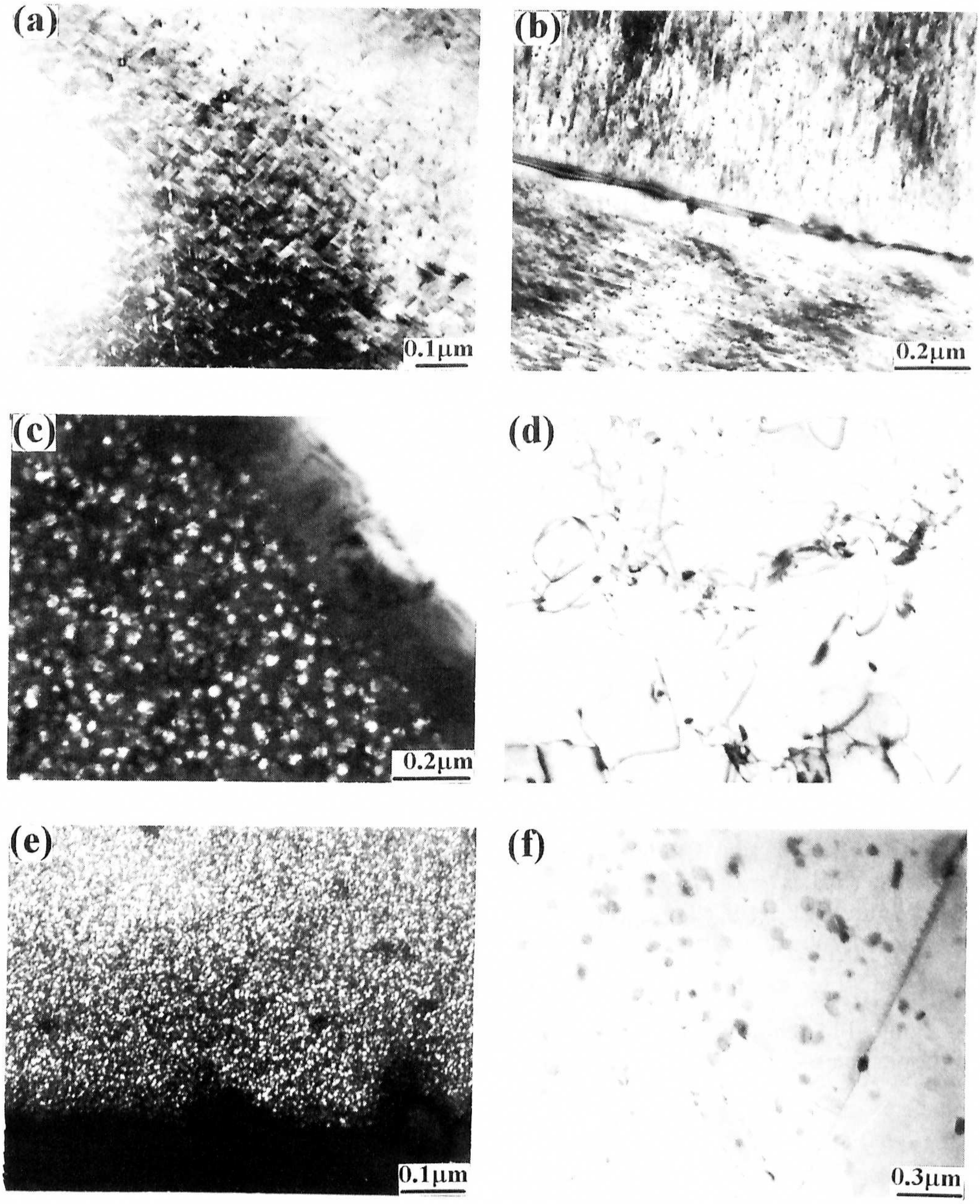

Figure 2 TEM microgragh of the alloys

(a) G.P. of Mg_2Si in Al-Mg-Si alloy aged for 24h at 443K (B=[112]$_{Al}$) (b) grain boundary in Al-Mg-Si alloy aged for 100h at 443K (B=[100]$_{Al}$) (c) δ′ phase in Al-Mg-Si-1.7Li alloy at after peak aging at 443K (B=[001]$_{Al}$, g=200) (d) LiSiAl particles in Al-Mg-Si-1.7Li alloy after peak aging at 443K (B=[011]$_{Al}$, g=200) (e) δ′ phase in Al-Mg-Si-2.6Li alloy after peak aging at 443K (B=[001]$_{Al}$, g=200) (f) LiSiAl particles in Al-Mg-Si-1.7Li alloy after peak aging at 443K (near [110]$_{Al}$)

Compare Fig.2(c, d) with Fig.2(e, f), as the Lithium content is increased from 1.7 to 2.6%, the volume fraction of δ′ and LiSiAl increases greatly at peak aging condition. No apparent PFZ's can be seen in alloy C.

3.3 Mechanical Properties

The results of tensile property measurements are presented in Table 2 for all three alloys after peak aging. The maximum tensile strength of 333 MPa was obtained for the base alloy A after aging for 24 hours whereas the maximum strength obtained for alloy B containing 1.7%Li was only 233 MPa after 80 hours at 443K. Alloy C possess the highest tensile strength, which was 385mpa, but its yield strength was 53 MPa lower than alloy A.

Table 2 Tensile properties of the peak aged alloys

Property	Alloy No.		
	A	B	C
σ_b, MPa	333	233	385
$\sigma_{0.2}$, MPa	304	144	251
δ_5, %	10.0	11.5	6.0

Alloy A shows normal elongation of 6000 series alloys with Si excess. The addition of 1.7%Li improves the elongation by 15%, while the addition of 2.6% Li drops it by 40% at peak aging condition.

3.4 Fractography

The fracture surfaces of the failed tensile samples with three alloy compositions have been examined. It can be seen from Fig. 3a that the fracture of alloy A is mainly composed of intergranular fracture and small amounts of dimples among the grains. The dimples on grain facets in high magnification photomicrographs (Fig. 3b) indicate that intergranular fracture is ductile in nature.

Fracture surfaces of alloy B (Fig.3c) shows completely ductile dimple fracture. Few particles can be seen in the dimples.

The fracture surface of alloy C (Fig.3d) shows mixed transgranular fracture and intergranular fracture modes. Amounts of large LiSiAl particles in dimples were found.

4. DISCUSSION

Aging of Al-Mg-Si alloys (6000 series) involves the nucleation, growth and transition of Mg_2Si. The precipitation sequence for the 6000 series alloys is:

$$\alpha(SSS) \rightarrow GP \rightarrow \beta'' \rightarrow \beta' \rightarrow \beta(Mg_2Si)$$

Alloy A (Al-0.6Mg-0.8Si) is a typical Al-Mg-Si alloy with high extent of excess in Silicon. Aging hardening is due to the precipitation of Mg_2Si after artificial aging. Silicon tends to precipitate on grain boundaries, thus promote the formation of PFZ's adjacent to the grain boundary. The presence of the soft PFZ imposes localised strain and precipitates on the grain boundary act as sites for microvoid formation. So the intergranular fracture occurs. The small dimples on grain facets conform the presence of PFZ's near the grain boundary.

As observed in TEM images, addition of Lithium in Al-Mg-Si alloys changes the precipitation behavior completely, and the ordered δ′ phase becomes the predominant precipitates in Li containing alloys.

The δ′ phase imposes limited strengthening on the Al matrix due to the small value of δ′/α misfit[7], furthermore the volume fraction of δ′ phase in alloy B is small because of the low content

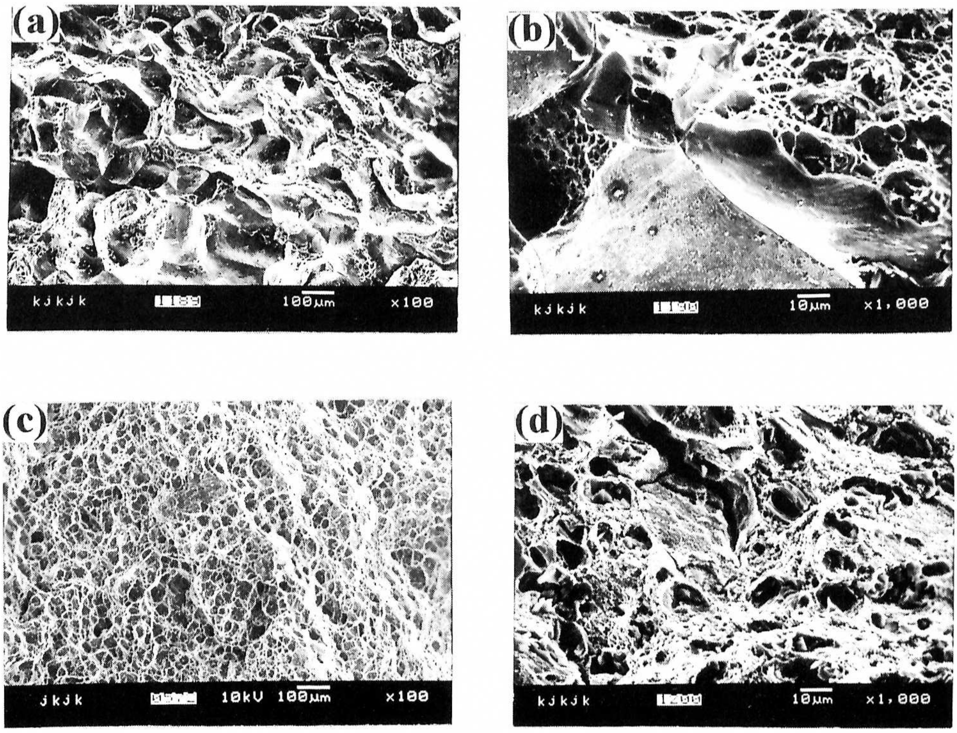

Figure 3 SEM micrograph of tensile fractures
(a) Al-Mg-Si alloy (b) high magnification of (a)
(c) Al-Mg-Si-1.7Li alloy (d) Al-Mg-Si-2.6Li alloy

of Li. This results in the very low hardness and strength of alloy B. The low supersaturation of Li is also responsible for the slow precipitation of δ′ and slow age-hardening response in alloy B.

Obvious PFZ′s forms in alloy B, due to the low vacancy density adjacent to grain boundaries. The limited free Li atoms prefer to precipitate within matrix where the vacancy density is high.

The addition of Li changes the phase diagram of Al-Mg-Si alloys, and LiAlSi ternary phase with cubic structure ($a = 5.94 \times 10^{-10}$m) forms [7]. They are large particles with nearly round shape in alloy B, and the number density of them is very low.

Fracture surfaces of alloy B shows completely ductile dimple fracture in spite of the presence of PFZ′s near grain boundaries in microstructure. The higher elongation compared with alloy A is associated with the very low matrix strength and the low linear density of precipitates on the grain boundary.

Like other convenient Al-Li alloy containing 2~3%Li, alloy C has a fast aging response due to the rapidly precipitation of δ′. The large volume fraction of δ′ accounts for the highest peak hardness and tensile strength of the three alloys.

The high content of Li promotes the precipitation of δ′ near the grain boundary, so no obvious PFZ′s were found there. Besides, the increase of free Li atom promotes the precipitation of LiSiAl particles. Compared with δ′ phase, however, LiSiAl particles are large and sparse, so it has little effect on strengthening.

The linear density of particles on the grain boundary in alloy C is a little higher than that in alloy B, in addition the precipitation of large amount of δ′ causes strong planar slip. This leads to earlier crack nucleation and premature intergranular fracture.

5. CONCLUSIONS

1. A lithium addition to Al-0.6Mg-0.8Si alloy, does not produce dual precipitation of the strengthening phases δ′ and β′. Coherent δ′ is the predominant strengthening phase in Li containing alloy. LiSiAl particles with small number density, distribute principally within matrix, and provide little hardening.
2. The alloy containing 1.7%Li shows very weak aging response. It shows a 100 MPa lower peak tensile strength and 15% higher elongation than the base alloy. The poor strength and improved elongation is related to the slowly precipitation of δ′ phase with low volume fraction.
3. The alloy containing 2.6% Li shows strong aging response. It has a 16% higher tensile strength but 40% lower elongation than the base alloy. This is related to the precipitation of δ′ phase with large volume fraction
4. The fracture surface of alloy containing 1.7%Li shows fully ductile dimple due to the low linear density of LiSiAl particles on the grain boundary and very weak strength of the matrix, while the fracture surface of alloy containing 2.6%Li shows mixed transgranular fracture and intergranular fracture, owing to the intense planar slip caused by excessive precipitation of coherent δ′ phase.

ACKNOWLEDGMENT

This work was funded by the Aerospace Science Foundation.

REFERENCES

[1] I. N. Flidlyander and A. G. Bratuhin: The 6th Aluminium-Lithium Conference, FRG 1991(VI): 35.
[2] E. S. Balmuth: The 4th International Conference on Aluminum Alloys, Atlanta, 1994(VIII): 82
[3] R. H. Graham and R. J. Rioja, et al.: in Ref. 1, 15
[4] Z. W. Huang, R. E. Smallman, et al.: Mater. Sci. and Tech., 1991(7), 205
[5] Z. W. Huang, R. E. Smallman and M. H. Loretto: in Ref. 1, 95
[6] Z. W. Huang, M. H. Loretto, et al.: Mater. Sci. and Tech., 1994(10), 869
[7] L. F. Mondolfo, Aluminum Alloys: Structure and Properties, London & Tonbridge, 1976
[8] S. F. Baumann and D. B. Williams: Aluminum-Lithium Alloys II, Monterey, 1983, 17